Yeast vacuoles fragment in an asymmetrical two-phase process with distinct protein requirements

Martin Zieger and Andreas Mayer
Département de Biochimie, Université de Lausanne, 1066 Epalinges, Switzerland

ABSTRACT **Yeast vacuoles fragment and fuse in response to environmental conditions, such as changes in osmotic conditions or nutrient availability. Here we analyze osmotically induced vacuole fragmentation by time-lapse microscopy. Small fragmentation products originate directly from the large central vacuole. This happens by asymmetrical scission rather than by consecutive equal divisions. Fragmentation occurs in two distinct phases. Initially, vacuoles shrink and generate deep invaginations that leave behind tubular structures in their vicinity. Already this invagination requires the dynamin-like GTPase Vps1p and the vacuolar proton gradient. Invaginations are stabilized by phosphatidylinositol 3-phosphate (PI(3)P) produced by the phosphoinositide 3-kinase complex II. Subsequently, vesicles pinch off from the tips of the tubular structures in a polarized manner, directly generating fragmentation products of the final size. This phase depends on the production of phosphatidylinositol-3,5-bisphosphate and the Fab1 complex. It is accelerated by the PI(3)P- and phosphatidylinositol 3,5-bisphosphate–binding protein Atg18p. Thus vacuoles fragment in two steps with distinct protein and lipid requirements.**

Monitoring Editor
Jean E. Gruenberg
University of Geneva

Received: May 7, 2012
Revised: Jun 29, 2012
Accepted: Jul 3, 2012

INTRODUCTION

Numerous organelles undergo membrane fission and fusion events during cell division or vesicular traffic or in response to changes in environmental conditions. Examples include the Golgi (Acharya *et al.*, 1998), mitochondria (Bleazard *et al.*, 1999), peroxisomes (Kuravi *et al.*, 2006), and lysosomes (Ward *et al.*, 1997). In the yeast *Saccharomyces cerevisiae*, the vacuole is the terminal component of the endocytic pathway. It serves as a lysosome-like hydrolytic compartment and as a major storage compartment and plays an important role in osmoregulation and ion homeostasis. Owing to its large size, this organelle represents a very good object with which to study membrane dynamics in vivo and in vitro (Kane, 2007).

On budding of yeast cells, the vacuole of the mother cell pinches off vesicles that migrate into the daughter cell, where they fuse to form a new vacuole (Weisman, 2003). Vacuolar morphology also changes in response to environmental conditions such as nutrient availability or the osmolarity of the medium. When exposed to hypertonic conditions, yeast cells divide their large vacuoles into numerous smaller ones, probably in order to readapt the surface-to-volume ratio of the compartment after the osmotic loss of water. The dynamin-like GTPase Vps1p is found on vacuoles (Peters *et al.*, 2004) and is implicated in the regulation of vacuolar fission and fusion. It bears the three classic dynamin domains, including a GTPase domain, a middle domain, and a GTPase effector domain (Rothman *et al.*, 1990; Vater *et al.*, 1992; Yu and Cai, 2004), but, unlike classic dynamins, it does not contain a PH domain. Dynamins can generate force and support many membrane fission processes (Hinshaw, 2000; Praefcke and McMahon, 2004). Vacuole fission also requires the proton pump activity of the vacuolar H^+-ATPase (Baars *et al.*, 2007) and the lipid phosphatidylinositol 3,5-bisphosphate ($PI(3,5)P_2$; Gary *et al.*, 1998; Bonangelino *et al.*, 2002). The concentration of $PI(3,5)P_2$ increases drastically upon osmotic stress. $PI(3,5)P_2$ in yeast is synthesized from phosphatidylinositol by two sequential phosphorylations by the phosphoinositide 3-kinase (PI 3-kinase) Vps34p and the phosphatidylinositol 3-phosphate (PI(3)P) 5-kinase Fab1p (Cooke *et al.*, 1998; Gary *et al.*, 1998). Fab1p carries a FYVE (Fab1, YOTB, Vac1, EEA1) domain that binds PI(3)P and localizes to the vacuole (Efe *et al.*, 2007). Fab1p kinase activity is regulated by three other proteins: Vac7p, Vac14p, and Fig4p (Bonangelino *et al.*, 2002; Dove *et al.*, 2002; Gary *et al.*, 2002). Vac7p and Vac14p were

This article was published online ahead of print in MBoC in Press (http://www.molbiolcell.org/cgi/doi/10.1091/mbc.E12-05-0347) on July 11, 2012.

Address correspondence to: Andreas Mayer (Andreas.Mayer@unil.ch).

Abbreviations used: CORVET, class C core vacuole/endosome tethering; PI(3)P, phosphatidylinositol-3-phosphate; $PI(3,5)P_2$, phosphatidylinositol-3,5-bisphosphate.

discovered in screens for mutants defective in vacuole inheritance (Gomes de Mesquita *et al.*, 1996; Wang *et al.*, 1996). They activate Fab1p. Fig4p dephosphorylates PI(3,5)P_2 to PI(3)P. Together with Vac14p, Fig4p is also necessary for Fab1 complex assembly (Gary *et al.*, 2002; Botelho *et al.*, 2008; Jin *et al.*, 2008), which could explain its second role in PI(3,5)P_2 synthesis. Deletion of VAC7, VAC14, or FAB1 leads to an enlarged vacuolar phenotype (Weisman, 2003). A link of the Fab1 complex to organelle transport into the bud during cell division is provided by Atg18p, a PI(3)P- and PI(3,5)P_2-binding protein that regulates Fab1 activity and binds Vac17p, an adaptor protein mediating the attachment of vacuoles to myosin V and actin (Tang *et al.*, 2003; Efe *et al.*, 2007).

Two additional proteins involved in vacuole fission are the CORVET subunit Vps3p (LaGrassa and Ungermann, 2005; Peplowska *et al.*, 2007) and the kinase Yck3p. Vacuoles are retained in the fragmented state by inhibiting fusion through a Yck3p-dependent phosphorylation of a subunit of the Rab-effector homotypic fusion and vacuole protein sorting complex, Vps41p (Cabrera *et al.*, 2009). Recently vacuole fragmentation has also been linked to nutritional conditions through the target of rapamycin complex (Michaillat *et al.*, 2012).

Vacuole fusion and fission change the surface-to-volume ratio of the organelle. Such adjustments are probably required upon changes in osmotic value, upon starvation, when the vacuolar hydrolytic enzymes are massively up-regulated, or for storage of reserve compounds, such as amino acids or polyphosphates (Kane, 2007). Here we used hypertonic stress to modify vacuole structure because it allows us to induce rapid, synchronous, and homogeneous vacuole fragmentation in a yeast population. This allowed us to study the process in real time.

Different scenarios can be invoked to explain how the vacuolar surface-to-volume ratio might be adapted to hypertonic stress (Figure 1A). It is unknown whether vacuoles divide equally in the middle, providing two fragmentation products of similar size, which might then undergo further rounds of fragmentation in order to produce the small vacuolar vesicles that are the final products of osmotically induced vacuole fragmentation. Alternatively, the organelle might fragment asymmetrically, producing small vesicles from a large central vacuole by a mechanism similar to budding. We address this question by time-resolved confocal microscopy of living yeast cells.

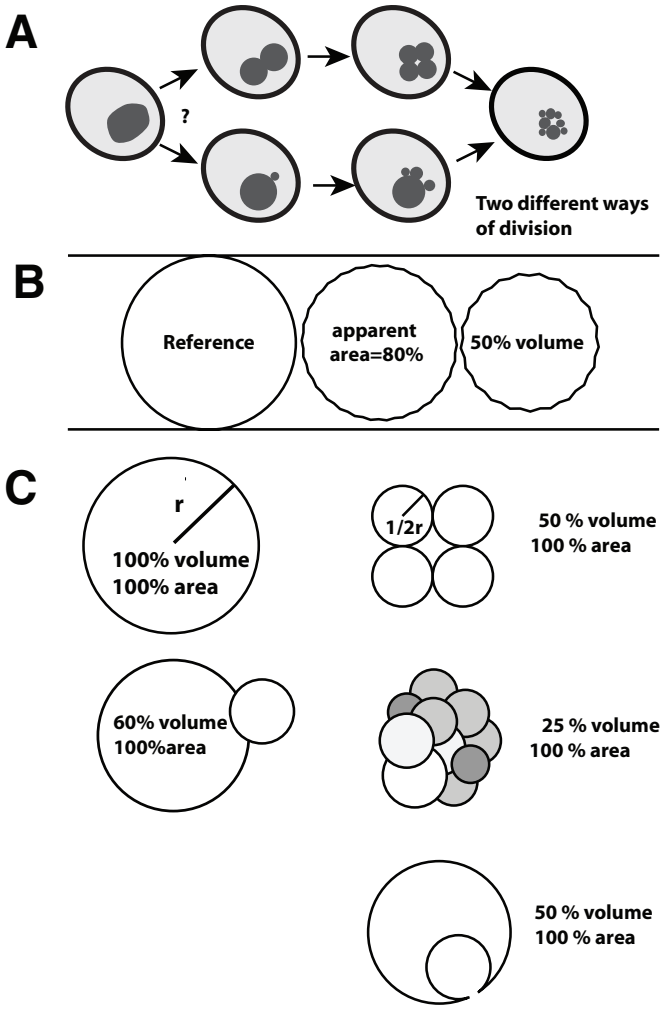

FIGURE 1: Examples of vacuolar morphologies and their surface-to-volume ratios. (A) Schematically drawn yeast cells illustrating symmetrical or asymmetrical vacuole division. (B) Relations between surface area, volume, and diameter. The three vesicles have the same surface. Membrane shriveling can reduce the surface area visible in the microscope because the shrivels cannot be resolved.
(C) Adaptation of the surface-to-volume ratio by division of spheres into equal-sized or unequal vesicles or by internalization of a vesicle.

RESULTS

Vacuole fragmentation is a polarized process occurring in two phases

Yeast vacuoles can be stained in living cells with the lipophilic dye FM4-64 (Vida and Emr, 1995). FM4-64–stained cells were immobilized on concanavalin A–coated chambered cover slides filled with medium. This attachment does not prevent normal growth and division of the cells (Supplemental Movie S1). After the start of image acquisition, vacuole fragmentation was induced on the microscope stage by supplementing the cell suspension with 0.5 M NaCl. Already seconds after this addition, the vacuoles shrank and began to form invaginations (Figure 2, A and B), leaving heteromorphic protrusions in their vicinity. The invaginations are distinct from vacuolar invaginations involved in micronucleophagy at nuclear–vacuolar junctions since neither the nuclear vacuolar junction protein Nvj1p (Pan *et al.*, 2000) nor the nucleolar marker Nop1p (Henriquez *et al.*, 1990; Dawaliby and Mayer, 2010) localized to them, and a strain deleted for NVJ1 is proficient for vacuole fragmentation. They are also unrelated to microautophagic invaginations because they could be observed in mutants that impair microautophagy, such as Δatg18 (see later discussion), Δatg5, and Δvtc4 (Muller *et al.*, 2000; Sattler and Mayer, 2000; Uttenweiler *et al.*, 2007).

The initial invagination phase, which lasted <1 min, was followed by a continuous remodeling of the vacuole. In this phase, the heteromorphic protrusions that were left in the vicinity of the invaginations rounded off and produced small, spherical structures that stayed attached to the remaining large central vacuole. This phase took 10–15 min to complete. After 15 min, all wild-type cells exhibited numerous spherical structures (Figure 2C). We preferentially use the background BJ3505 because it provides big cells and vacuoles that are well suited for light-microscopic analysis. Furthermore, its *pep4* mutation reduces proteolytic artefacts in biochemical fractionations, which will be performed in future analyses of the fragmentation reaction. Cells from other strain backgrounds behaved similarly as BJ3505 (Figure 2D), indicating that the mode of vacuole remodeling is not strain specific. To confirm our observations from light microscopy, we recorded electron micrographs of yeast cells at

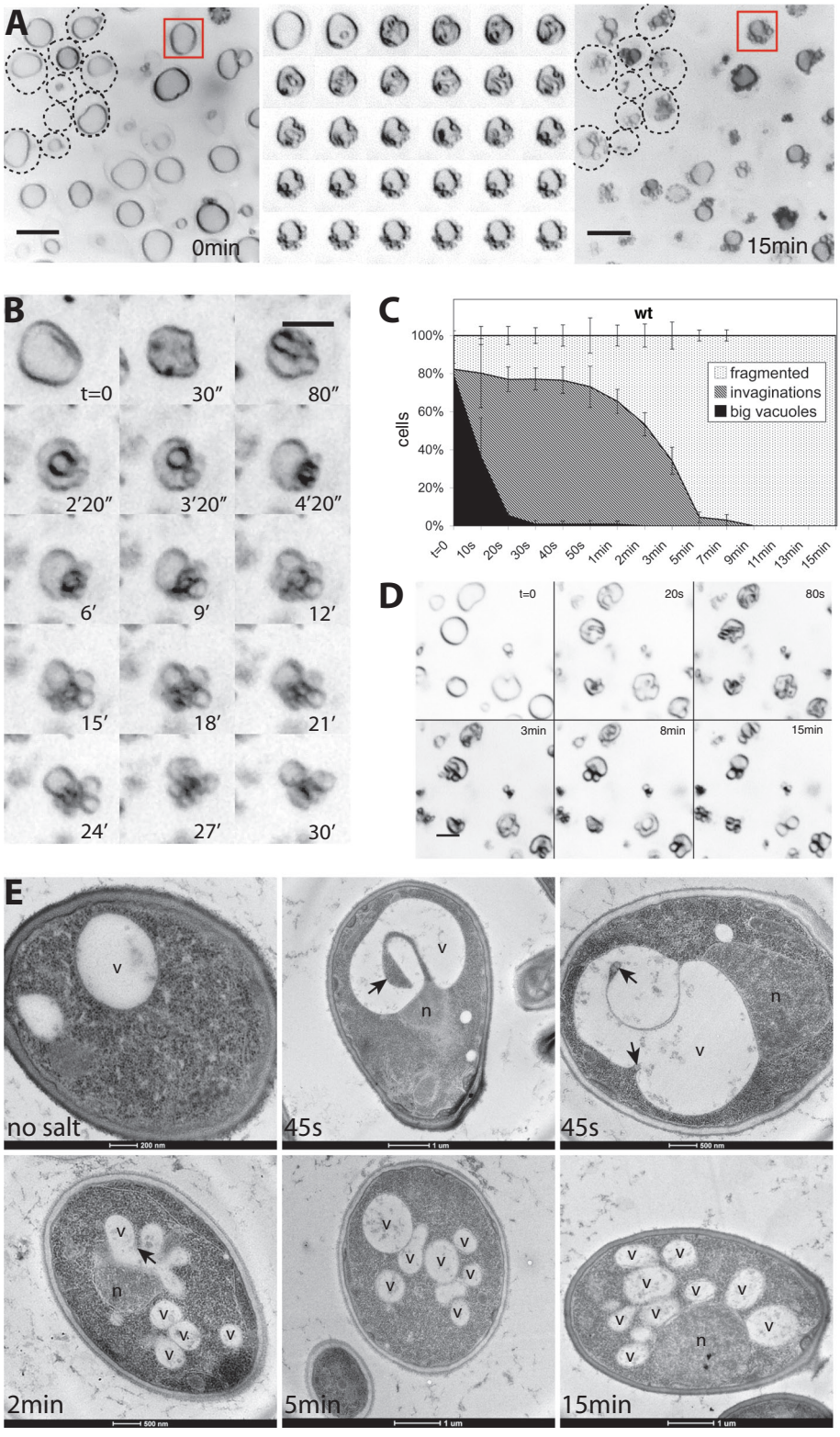

FIGURE 2: Remodeling of invaginated vacuoles into vesicles. Vacuole fragmentation was induced in FM4-64–stained wild-type (BJ3505) cells by addition of 0.5 M NaCl. (A) Vacuole structure of a group of cells before (left) and 15 min after salt addition (right). The cell perimeters for some cells are indicted by dashed lines. Middle, a magnified view of the vacuole marked by a red square. Images of this vacuole were taken every 20 s during the 10 min after salt addition. Scale bars, 2 μM. (B) Maximum-intensity projection of optical sections of a single vacuole during fragmentation, covering 4 μM in the *z*-direction. (C) Quantification of vacuole fragmentation in BJ3505 in vivo. Cells were scored according to their vacuolar morphology at different time points after salt addition. We distinguished cells with big intact vacuoles without invaginations, cells with vacuolar invaginations of various sizes, and cells with mainly fragmented vacuoles. Three independent image series were analyzed for each time point. (D) Vacuolar fission in CRY1 wild-type cells, a protease-competent strain with vacuoles of similar size as BJ3505. Cells were stained with FM4-64 and imaged at the indicated times after salt addition. (E) Electron micrographs of BJ3505 cells subjected to high-pressure freezing and freeze substitution at different time points after salt shock. Arrows mark invaginations. v, vacuole; n, nucleus.

different times after osmotic shock (Figure 2E). At 45 s past the salt shock, most vacuoles exhibited invaginations of various sizes, similar to what was seen before by fluorescence microscopy. After 2 min, cells with smaller spherical structures became more numerous, and after 5 min, few invaginations remained, and small, spherical structures predominated. At the 15-min time point, all cells showed exclusively small round vacuolar structures.

Next we tested whether the spherical structures that appeared were products of true vacuole fragmentation, that is, vacuolar vesicles separated from the rest of the organelle. They might as well represent vacuolar invaginations or evaginations that were optically sectioned, a process that would also yield circular profiles. In addition, lumenal vesicles that pinched off into the interior of the vacuole could result in similar images in the light microscope. Owing to the limited resolution of the confocal microscope, we could not unequivocally address this problem by three-dimensional reconstruction. Therefore we used a strain expressing a cytosolic version of green fluorescent protein (GFP), which would fill any invagination of the vacuolar membrane and also lumenal vesicles generated from it. We found examples for clearly identifiable vacuolar invaginations that were longitudinally sectioned and accordingly colored by GFP, confirming the validity of the approach. The large majority of spherical structures generated from the invaginated vacuoles, however, did not show lumenal GFP staining (Figure 3A). Therefore these spherical structures retained the outside-out configuration of the vacuolar membrane. That these newly formed structures were completely detached from the original vacuole could be demonstrated by fluorescence recovery after photobleaching (FRAP) analysis. We used a strain expressing a GFP fusion of the membrane-integral vacuolar V-ATPase subunit Vph1p (Figure 3, B and C). If one of the vesicles

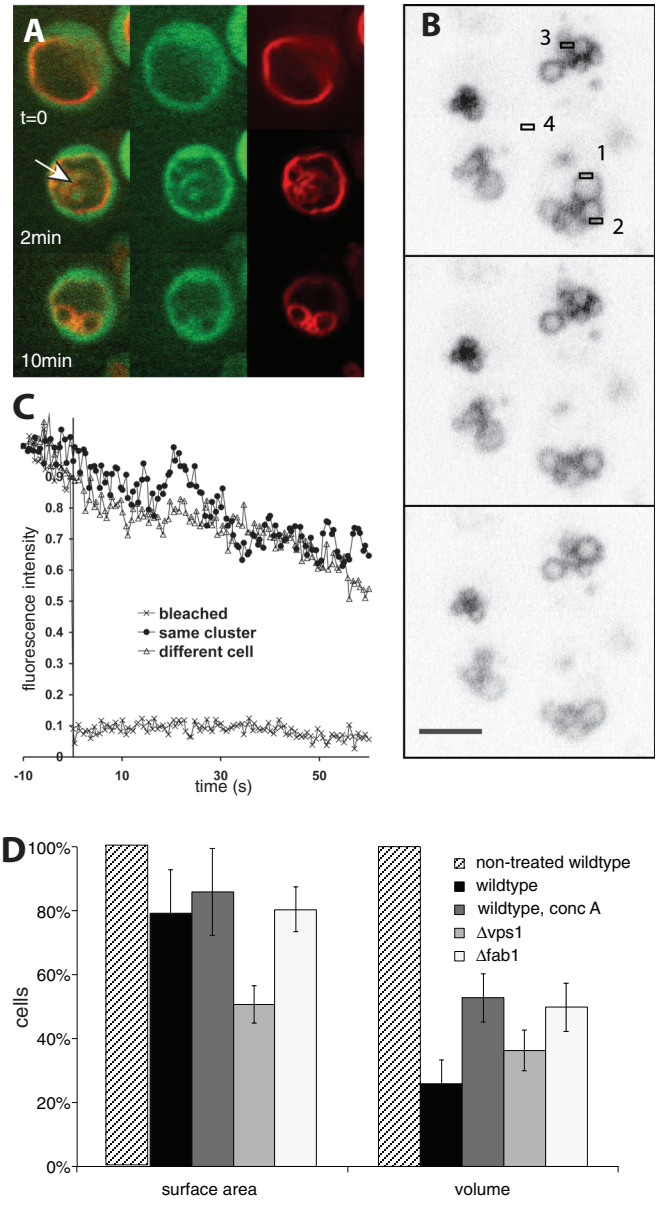

FIGURE 3: Newly formed structures are detached vesicles rather than optically sectioned vacuolar lobes. (A) Wild-type cells (CRY1) expressing soluble GFP (green channel) were stained with FM4-64 (red channel) and observed after salt shock. The arrow marks intravacuolar structures filled with cytosolic GFP. (B) FRAP analysis of a cell expressing Vph1-GFP (Peters *et al.*, 2001). Bleaching was induced by a 200-ms laser pulse at $t = 0$ s in area 1. (C) Fluorescence was traced over time in the following areas of the field in B: from the bleached area (area 1), from the same vacuole cluster (area 2), and from vacuoles of another cell (area 3). The background signal (area 4) was averaged over the 70 s and subtracted from all other signals. Signals are normalized to the value observed 10 s before salt addition ($F_{(-10\ s)} = 1$). (D) Yeast cells carrying the indicated mutations or treated with concanamycin A were incubated for 15 min with 0.5 M NaCl and analyzed by serial optical sectioning in a confocal microscope. We calculated the apparent vacuolar volume and membrane surface area after averaging the measured diameters for every single vesicle analyzed ($n = 15$). Vacuoles were approximated as spheres.

from a freshly fragmented cluster of vacuoles was bleached with a laser, its fluorescence signal did not recover by delivery of protein from the other vesicles in vicinity. Correspondingly, the fluorescence signal of these neighboring vacuoles was retained during the laser pulse, as well as after the photobleaching. We only observed a slow, constant bleaching that was common to all fluorescent structures and due to continued image acquisition. These data suggest that the spherical structures formed after the osmotic challenge represent vacuolar vesicles completely separated from each other.

We measured the surface and volume of the vacuoles before and after the reaction. Their volume decreased by 75% (Figure 3D), whereas the apparent surface area remained almost constant and decreased only by 20%. The apparent loss of surface might be due to the limited resolution of the light microscope, which precludes resolution of small tubular or vesicular membrane structures adjacent to a vacuolar boundary membrane. In addition, membrane shriveling (Figure 1B) can reduce the apparent vacuole surface. We could observe vacuole shriveling in a low percentage of cells and suppose that it might remain undetectable in the majority of the cases if it is not sufficiently pronounced.

The initial invagination phase requires V-ATPase activity and the dynamin-like GTPase Vps1p

The proton pump activity of the V-ATPase and the resulting proton gradient across the vacuolar membrane are required for vacuole fragmentation (Baars *et al.*, 2007). We used a Δvma1 strain, which lacks a catalytic subunit of the V-ATPase, in order to test which step of vacuole fragmentation depends on the vacuolar proton gradient. Δvma1 cells showed a single large, round vacuole (Figure 4A). On hypertonic shock, vacuoles from Δvma1 cells did not show any deep invaginations at the 2-min time point, when they are highly prominent in wild-type cells (Figure 2A). The vacuoles showed only a slight shrinking and shriveling of the vacuolar membrane, leading to shallow indentations that rapidly disappeared during the next 10–15 min without producing vacuolar fragments. Even those shallow invaginations were much less frequent than the pronounced invaginations in the wild type. Owing to the vacuolar acidification defect these mutants exhibit weaker FM4-64 staining of the vacuolar boundary membrane and an enhanced lumenal background staining, probably reflecting the intravacuolar accumulation of multivesicular body (MVB) vesicles (Wurmser and Emr, 1998). We also tested the effect of pharmacological suppression of V-ATPase function in wild-type cells. This more acute treatment can circumvent secondary effects resulting from the constitutive absence of V-ATPase activity in deletion mutants (Kane, 2007). In addition, short treatment of wild-type cells with a potent inhibitor of the vacuolar H^+-ATPase, concanamycin A (Drose and Altendorf, 1997), blocked deep vacuolar invagination after salt shock and permitted only shallow, less frequent indentations (Figure 4B). Quantification over time illustrates this fact (Figure 4C). This suggests that the electrochemical potential over the vacuolar membrane is necessary for the deep vacuolar invaginations that precede fragmentation. In line with this, inactivation of V-ATPase also impedes the reduction of vacuolar volume upon hypertonic shock (Figure 3D).

The dynamin-like GTPase Vps1 is necessary for both vacuole fragmentation and fusion in yeast (Peters *et al.*, 2004; Michaillat *et al.*, 2012). We tested which phase of vacuole fragmentation was affected by this protein. Cells from a Δvps1 deletion strain show a large, round central vacuole surrounded by smaller vesicles. When Δvps1 cells were exposed to a salt shock, their large, round vacuoles did not fragment (Figure 5, A and B) and showed reduced shrinking. Their invaginations were much shallower and less numerous than those in wild-type cells (Figure 5, A–C). They formed more slowly, with a half-time of 20 instead of 10 s for the wild type. They were also unstable and disappeared within a few minutes (Figure 5D).

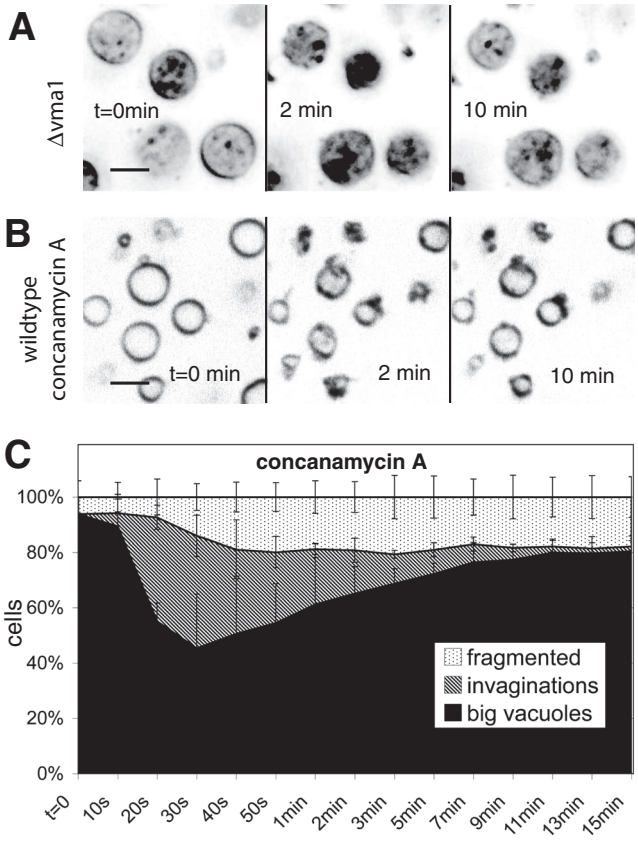

FIGURE 4: Necessity of the vacuolar proton gradient for vacuole invagination. Cells were stained with FM4-64 and imaged at the indicated time points after addition of 0.5 M NaCl. (A) A Δvma1 strain. (B) Wild-type (BJ3505) cells treated with concanamycin A for 60 min. (C) Quantification of morphological changes over time for vacuoles of concanamycin A–treated wild-type cells. Compare with the graph for nontreated cells in Figure 2C.

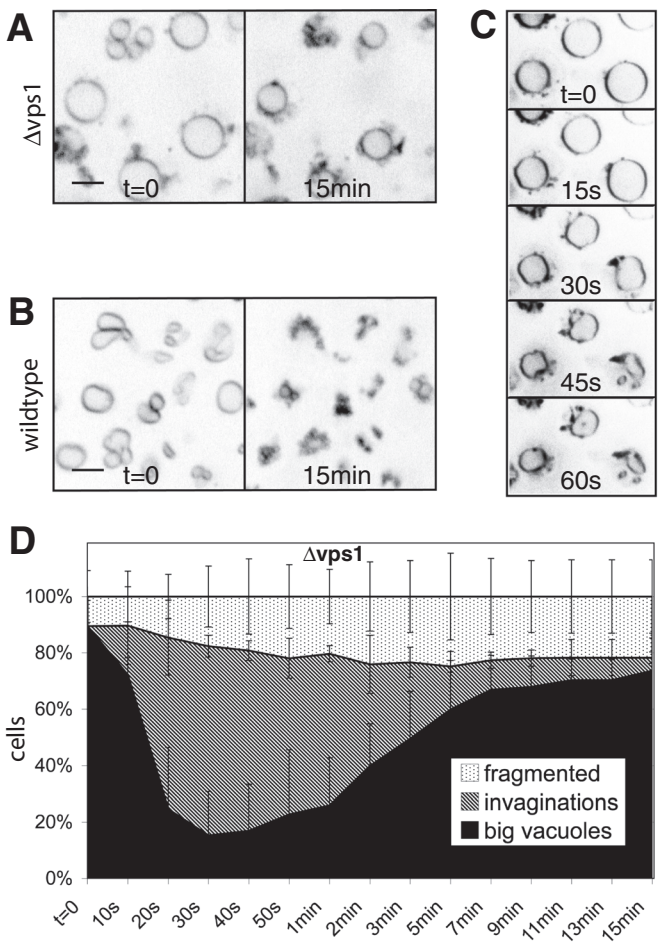

FIGURE 5: Influence of Vps1p on vacuolar invagination. Cells stained with FM4-64 were observed before and 15 min after addition of 0.5 M NaCl for (A) Δvps1 and (B) wild-type (BJ3505) cells. (C) Sequence showing the first minute after salt shock of wild-type cells imaged at a rate of one frame per 15 s. (D) Quantification of morphological changes over time for vacuoles of Δvps1 cells. Compare with the graph for wild-type cells in Figure 2C.

Δvps1 vacuoles did not produce normal-sized vacuolar fragmentation products from their large central vacuoles upon salt treatment, but they showed additional, poorly resolvable tubulovesicular evaginations emanating from the surface of the large central vacuole. These data suggest that Vps1p already influences the invagination of the vacuolar membrane. This early defect interferes with attempts to assay a contribution of Vps1p to the subsequent scission of vacuolar fragments, which we nevertheless expect to exist, due to the well-characterized fission activities of dynamin-like GTPases (Schmid and Frolov, 2011).

The phosphatidylinositol-3-phosphate 5-kinase Fab1p is required for vesiculation but not for invagination

The level of PI(3,5)P_2 increases up to 20-fold upon osmotic stress, and PI(3,5)P_2 regulates vacuolar morphology. PI(3,5)P_2 is produced by a protein complex of the catalytic subunit Fab1p and its regulatory subunits Vac7p, Vac14p, and Fig4p. Cells deleted for the PI(3,5)P_2-producing kinase Fab1 show single enlarged vacuoles and are defective in vacuole inheritance and vacuole fragmentation (Yamamoto *et al.*, 1995; Wang *et al.*, 1996; Dove *et al.*, 1997; Cooke *et al.*, 1998; Gary *et al.*, 1998; Bonangelino *et al.*, 2002; Jin *et al.*, 2008). On a salt shock, vacuoles of Δfab1 cells still formed deep invaginations at a high frequency, but they could not form vacuolar fragments (Figure 6, A and B). Unlike the labile invaginations in Δvps1 cells, the invaginations in Δfab1 cells persisted for the entire observation period of 15 min (Figure 6E). After prolonged incubation, the initial invaginations rounded up and formed spherical structures in the interior of the vacuole. These structures contain engulfed cytosolic material, as demonstrated by their staining with cytosolic fluorescent probes such as soluble GFP or $FYVE_2$-GFP (see later discussion). They were mobile inside the vacuoles, suggesting that they had detached from the boundary membrane. Similarly, cells lacking the Fab1p activator Vac7p, which are also defective for vacuole fragmentation (Gary *et al.*, 1998, 2002), showed long-lived invaginations, but intravacuolar spherical structures were less frequent (Figure 6C). In addition, a Δvac14 mutant (Bonangelino *et al.*, 2002; Dove *et al.*, 2002; Jin *et al.*, 2008) showed a qualitatively similar defect in the formation of vacuolar fragments, which was, however, less pronounced than in Δfab1 cells (Figure 6D). The less pronounced effects of the noncatalytic subunits of the Fab1 complex are likely due to the persistence of small amounts of PI(3,5)P_2 in these strains (Efe *et al.*, 2007).

We also analyzed cells lacking the PI 3-kinase Vps34p (Schu *et al.*, 1993), which produces the substrate for Fab1p. Vps34p exists in two PI 3-kinase complexes—an autophagosomal complex I and

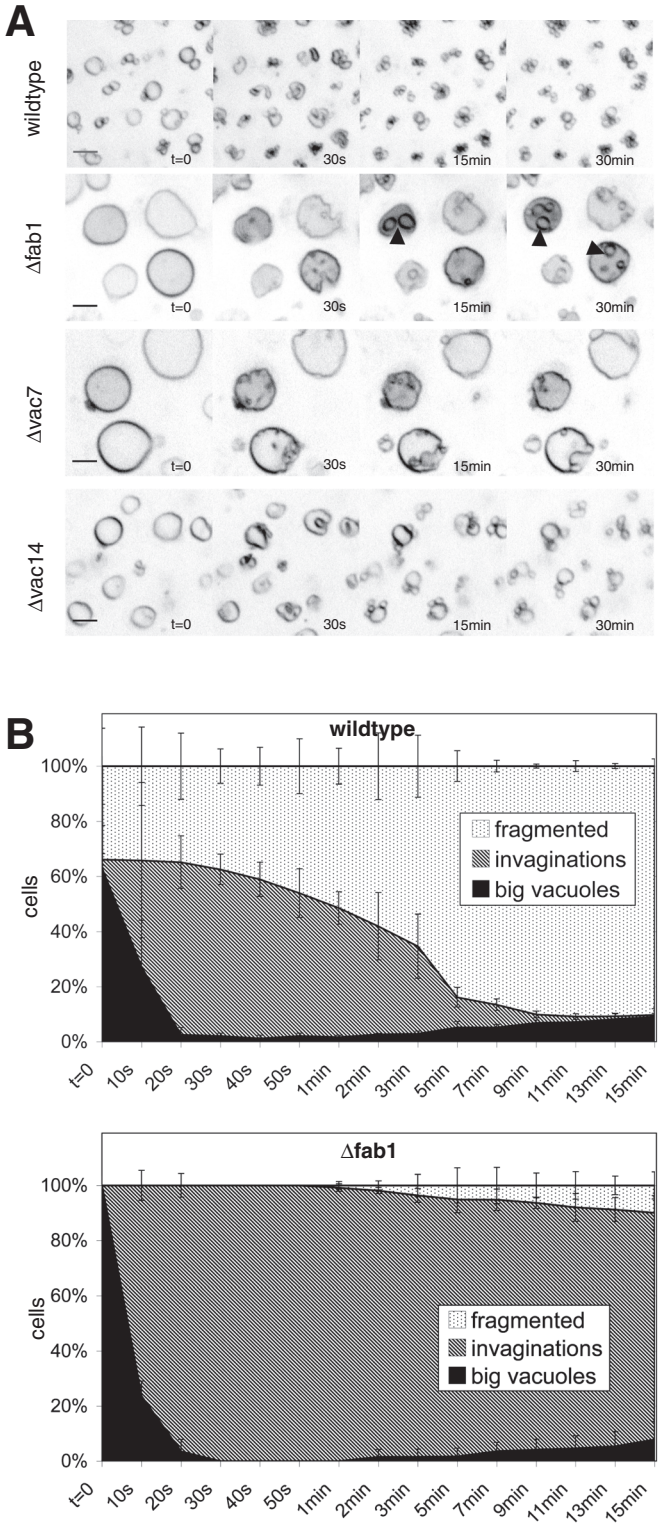

FIGURE 6: Defects of vacuolar fragmentation in mutants lacking Fab1 complex subunits. Cells were stained with FM4-64 and imaged at the indicated times after salt addition. (A) Wild-type (DKY6281). Δfab1 (arrowheads mark intravacuolar structures), Δvac7, and Δvac14 cells. (B) Quantification of morphological changes over time for vacuoles of wild-type and of Δfab1 cells.

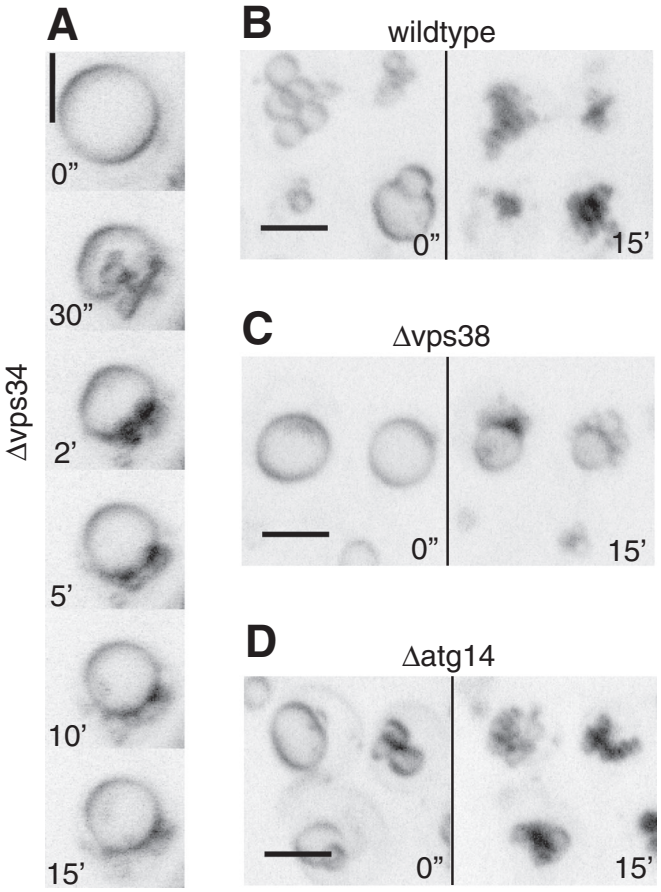

FIGURE 7: Influence of mutations in different PI 3-kinase complex I and II subunits. Cells were stained with FM4-64 and imaged at the indicated times after salt addition. Pictures are maximum-intensity projections of five *z*-sections with 0.5-μm spacing. (A) Δvps34, (B) wild type, (C) Δvps38, (D) Δatg14.

the endosomal/vacuolar complex II (Kihara *et al.*, 2001; Burda *et al.*, 2002). The vacuoles in Δvps34 cells did not fragment (Figure 7A). Deletion of the gene for the endosomal/vacuolar complex II subunit Vps38p (Figure 7C) significantly reduced salt-induced vacuole fragmentation, whereas deletion of the gene for the autophagosomal complex I subunit Atg14p (Tsukada and Ohsumi, 1993; Kametaka *et al.*, 1998; Kihara *et al.*, 2001) had no effect (Figure 7D). Closer inspection of the fragmentation process revealed that Δvps34 cells showed pronounced vacuolar invaginations upon salt treatment. Although the vacuoles in both Δvps34 and Δfab1 cells did not fragment, the invaginations in Δvps34 decayed during the 15 min of observation, whereas in Δfab1 cells they remained stable. Δfab1 cells not only fail to produce PI(3,5)P_2 but also accumulate increased levels of PI(3)P, suggesting that accumulating PI(3)P might stabilize vacuolar invaginations and that its metabolization into PI(3,5)P_2 might be needed to vesiculate the membrane.

This hypothesis is consistent with results from our attempts to localize PI(3)P. Membranes containing PI(3)P can be labeled in living cells with a probe containing two PI(3)P-binding FYVE domains from the human Hrs protein fused to GFP (Gillooly *et al.*, 2000). Expression of this probe in Δfab1 cells brightly stains foci on the vacuolar boundary membrane and vacuolar invaginations (Figure 8A, arrowheads). As invaginations form during fragmentation, those foci move to invaginated regions and concentrate there. Wild-type cells also show $FYVE_2$-GFP foci on the vacuolar boundary membrane and in invaginated regions upon salt addition. In contrast to the persistent signal on the intravacuolar structures in Δfab1 cells, however, the foci in wild-type cells dissociated again in the course of fragmentation

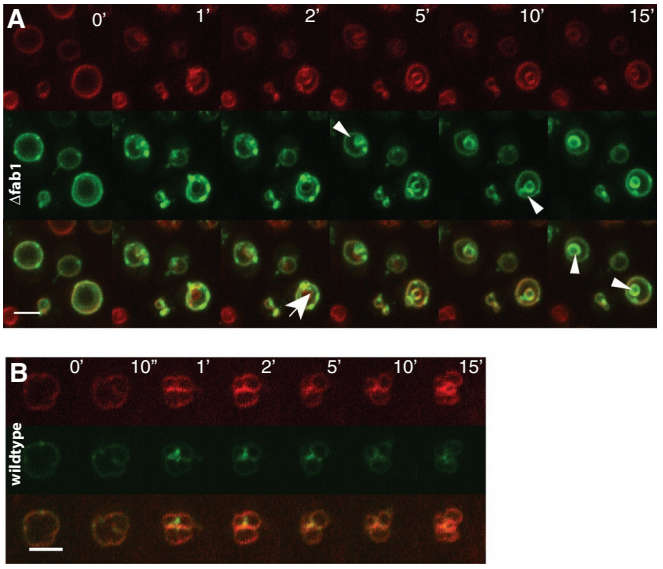

FIGURE 8: Localization of $FYVE_2$-GFP during vacuole fragmentation. Cells were stained with FM4-64 (red) and imaged at the indicated times after salt addition for FM4-64 (red) and GFP (green) fluorescence. (A) Δfab1 (BY4741) expressing $FYVE_2$-GFP. Arrowheads mark accumulations of the probe on intravacuolar structures. The arrow marks an invagination that acquires FYVE-GFP only after its formation. (B) Wild-type (BY4741) cells expressing $FYVE_2$-GFP.

(Figure 8B). This suggests a transient enrichment of PI(3)P on invaginating regions of the vacuoles during fragmentation.

In search of potential effectors of PI(3)P and $PI(3,5)P_2$, we tested proteins known to bind these lipids. Atg18p is a vacuole-associated protein that binds $PI(3,5)P_2$ with high affinity and negatively regulates $PI(3,5)P_2$ production (Dove *et al.*, 2004, 2009; Stromhaug *et al.*, 2004; Efe *et al.*, 2007). Cells lacking Atg18p show a drastically increased steady-state level of $PI(3,5)P_2$ and enlarged vacuoles. We observed that in Δatg18 cells vacuole fragmentation is significantly delayed (Figure 9, A and B). Δatg18 differs from other mutants affecting the Fab1 complex in that it displays enlarged vacuoles and vacuolar fragmentation problems despite the fact that it shows no reduction in $PI(3,5)P_2$ at the whole-cell level. Therefore we tested whether Fab1p might be mislocalized in a Δatg18 cell, which might allow synthesis of $PI(3,5)P_2$ but not in the place where it is required. We generated cells expressing a Fab1p-GFP fusion as the sole source of Fab1, either in the presence or absence of ATG18. In both cases, Fab1p-GFP showed the same localization to the vacuolar rim. It was concentrated in an inhomogeneous manner on the vacuoles, confirming earlier observations (Bonangelino *et al.*, 2002).

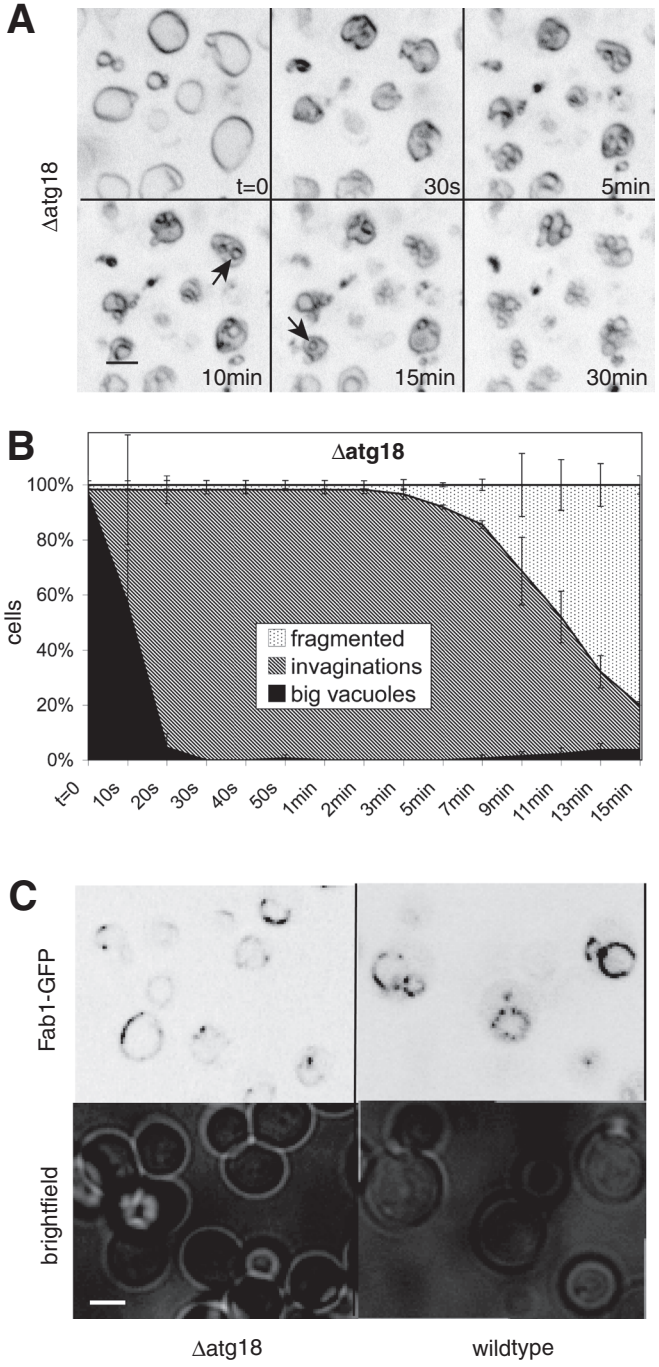

FIGURE 9: Vacuole fragmentation in Δatg18 cells is retarded. (A) Δatg18 (BJ3505) cells were stained with FM4-64 (red) and imaged at the indicated times after salt addition. Arrows mark intravacuolar spherical structures. (B) Quantification of the fragmentation of Δatg18 vacuoles. Compare with the graph for wild-type cells in Figure 2C. (C) Localization of Fab1p in Δatg18 cells. Wild-type and isogenic Δatg18 cells carrying Fab1-GFP were grown logarithmically in YPD. Fab1-GFP localization was analyzed by confocal fluorescence microscopy.

DISCUSSION

On hypertonic treatment, vacuoles shrink within seconds, probably to compensate for the water efflux from the cytosol to the surrounding medium. Shrinking is accompanied by tubular invaginations of the vacuole. Vesicles are formed from the finger-like protrusions remaining between them. These observations raise several interesting questions. First, why do vacuoles fragment at all in an active, protein- and lipid-dependent manner? It appears that many vacuolar functions, such as hydrolytic degradation or the storage of polyphosphates, amino acids, and polyamines, might also work in a shrunken organelle that is not round. A major difference between a deflated and an inflated state of an organelle is the tension of its membrane. Shrinking changes the surface-to-volume ratio and eliminates membrane tension. Fragmenting the organelle into multiple smaller copies readjusts the surface-to-volume ratio and hence allows reestablishment of tension of the vacuolar boundary membrane. Membrane tension can influence the activity of channel and transport proteins (Hamill and Martinac, 2001). Vacuoles contain

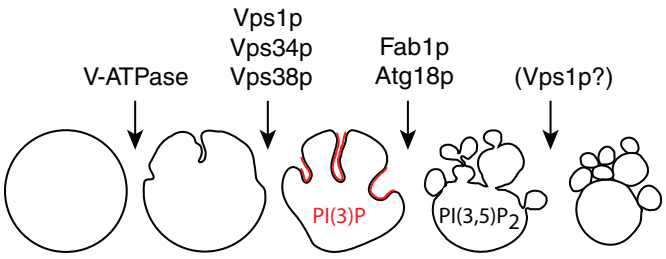

FIGURE 10: Schematic representation of the phases of hypertonically induced vacuole fragmentation and the involvement of various fragmentation factors at different phases.

numerous channels and transporters, which are crucial for its function in storage and release of various compounds. Some of them might be affected by membrane tension, for example, the vacuolar Ca^{2+} channel Yvc1p, which releases Ca^{2+} upon hypertonic shock (Chang *et al.*, 2010). In addition, membrane tension may be necessary to allow vesicular traffic to the organelle. Fusion between vacuoles and vesicular transport to them depend on the Rab-GTPase Ypt7p (Wada *et al.*, 1992; Wichmann *et al.*, 1992; Haas *et al.*, 1995; Mayer and Wickner, 1997), and the function of Ypt7p is influenced by membrane tension (Brett and Merz, 2008). Thus it is likely that vacuolar membrane tension needs to be maintained to sustain vacuolar membrane trafficking routes.

A second interesting aspect is the fact that fragmentation happens asymmetrically. It immediately produces fragmentation products of the final size rather than proceeding through a series of equal divisions to generate vesicles of increasingly smaller size (Figure 1). Separating small vesicles with a high surface-to-volume ratio should permit more rapid readjustment of this ratio and the regaining of functionality of the compartment because already the first fragmentation products will possess a drastically increased surface-to-volume ratio.

A third interesting aspect is the involvement of the different fragmentation factors at different phases of the process (Figure 10). Osmotically induced invaginations of the vacuolar membrane might be taken as a passive shape change dictated by the efflux of water and loss of volume, but this seems not to be the case. Invagination can be suppressed by deletion of either the V-ATPase or the dynamin-like GTPase Vps1p. Salt stress stimulates rapid assembly of the V_1 and V_0 sectors of the V-ATPase (Li *et al.*, 2012). The resulting augmented electrochemical gradient across the vacuolar membrane might directly affect distribution and properties of vacuolar lipids in order to support its large-scale deformations. Changes in the electrochemical membrane potential can directly induce transbilayer lipid asymmetry (Farge and Devaux, 1992; Mui *et al.*, 1995; Sackmann and Feder, 1995) and lateral phase separations of lipids (Schaffer and Thiele, 2004). Such changes are sufficient not only to tubulate pure two-phase lipid systems, but also to allow vesicle scission from them (Julicher and Lipowsky, 1993; Lipowsky, 1995).

A deficiency in proton pumping could also affect the vacuolar membrane by influencing the turnover of vacuolar contents. The major vacuolar compounds are polyphosphates, which are synthesized by the vacuolar VTC complex (Hothorn *et al.*, 2009) and can form up to 30% of the dry weight of yeast (Liss and Langen, 1962). Polyphosphates influence vacuolar membrane dynamics, as illustrated by their roles in vacuolar invagination during microautophagy (Uttenweiler *et al.*, 2007) and in vacuole fusion (Muller *et al.*, 2002, 2003). Their turnover depends on an endopolyphosphatase that must be matured by vacuolar hydrolases, a process that probably depends on vacuolar acidification (Sethuraman *et al.*, 2001; Shi and Kornberg, 2005). Polyphosphates contain up to hundreds of phosphate residues, are highly negatively charged, and form complexes with Ca^{2+}, Mn^{2+}, Mg^{2+}, basic amino acids, and other monovalent cations (Rao *et al.*, 2009). It is conceivable that polyphosphates might also associate with and cluster charged lipids, either by direct binding or by ionic bridges via bivalent cations. Because uptake and turnover of most vacuolar compounds depend on H^+-driven transporters (Kane, 2007), perturbation of the proton gradient could interfere with vacuolar invagination by affecting vacuolar ion balance and lipid distribution.

We observed an unexpected early role for Vps1p in fragmentation since Δvps1 vacuoles do not show the large invaginations that can be observed in wild-type cells. The membrane in invaginated areas is negatively curved, but dynamin-like proteins bind to membrane areas of high positive curvature and can thereby promote tubulation and scission of membranes (Roux *et al.*, 2010; Schmid and Frolov, 2011). If the role of Vps1p for forming the invagination was related to its binding to positively curved regions, it could only affect the rim of a forming indentation of the vacuolar boundary membrane. Here the membrane is positively curved. Vps1p might thus stabilize the rims of the invaginating structures. In this way, Vps1p should also be enriched at the tips of the remaining finger-like structures that can be observed between invaginations, that is, at the sites where scission of the final fragmentation products occurs. We could not test this model directly by microscopy because we were not able to produce tagged versions of Vps1p that showed a normal invagination pattern, although our tagged versions were functional for other aspects of Vps1p activity, such as endocytosis or vacuole fusion (Peters *et al.*, 2004; Smaczynska-de Rooij *et al.*, 2010). Attempts to localize Vps1p by immuno–electron microscopy have not succeeded. Our observation of a role of Vps1 in the formation of invaginations is consistent with observations of Hyams and coworkers in *Schizosaccharomyces pombe*, who ascribed to Vps1p a function in tubulating vacuoles (Rothlisberger *et al.*, 2009). In *S. pombe*, vacuole scission required an additional dynamin-like GTPase, Dnm1p. In *S. cerevisiae*, however, we observed that vacuole fragmentation in a Δdnm1 mutant occurs normally (unpublished data).

The locally appearing tubules are probably accompanied by changes in the lipid phase in those areas. Our study illustrates this for one lipid, PI(3)P. On hypertonic shock, the amounts of $PI(3,5)P_2$ on the vacuole increases 10- to 20-fold (Dove *et al.*, 1997; Bonangelino *et al.*, 2002). In addition, the levels of PI(3)P rise, although more moderately. Live-cell imaging of a strain deleted for the PI(3)P 5-kinase Fab1p shows that the mutant vacuoles invaginate even more vigorously than those of wild-type cells, whereas the actual formation of new vesicles is drastically reduced and delayed. Instead, the deep invaginations evolve into spherical structures that accumulate inside the vacuole. We consider those as degenerated or "frustrated" invaginations. They show a high level of PI(3)P. Because cells lacking Fab1p accumulate PI(3)P, these spherical invaginated structures may result from the hyperaccumulation of PI(3)P due to the inability to convert it into $PI(3,5)P_2$. In line with this, a Δvps34 strain that no longer produces PI(3)P does not show this increased invagination activity and does not accumulate intravacuolar spherical structures. We hypothesize that PI(3)P and $PI(3,5)P_2$ could act sequentially in vacuole fragmentation. PI(3)P, produced from PI 3-kinase complex II, might stabilize invaginations, and its conversion to $PI(3,5)P_2$ might induce the subsequent fission of vesicles from the membrane protrusions remaining between the invaginations. A surplus in PI(3)P might recruit proteins that induce negative curvature and stabilize the invaginations, eventually leading to the observed spherical structures if PI(3)P is not converted into $PI(3,5)P_2$.

The formation of PI(3)P and PI(3,5)P_2 from PI might itself influence membrane curvature, but the change in the head group is rather small. We consider it as more likely that these lipids operate by recruiting lipid-binding proteins, which then help to shape the membranes. A candidate for such a factor is Atg18p, a PI(3,5)P_2-binding protein that regulates Fab1p activity (Dove *et al.*, 2004; Efe *et al.*, 2007). Atg18p is recruited to the vacuolar membrane after hypertonic shock. Δatg18 cells fragment their vacuoles less well than wild-type cells, although they have even more PI(3,5)P_2. In other mutants affecting the Fab1 complex the situation is inverse, that is, their fragmentation defects correlate to strong reductions in PI(3,5)P_2 levels. The fragmentation defect of Δatg18 cells might result from the perturbations caused by the increased PI(3,5)P_2 level. This, however, seems unlikely because fab1-5 mutants, which show a similar increase in PI(3,5)P_2 as Δatg18 cells, have hyperfragmented vacuoles (Gary *et al.*, 2002; Efe *et al.*, 2007). Thus it is more likely that Atg18p supports the transition from invaginated to fragmented vacuoles independent of its influence on the conversion of PI(3)P to PI(3,5)P_2, perhaps via its interaction with PI(3,5)P_2 and resulting influences on membrane curvature.

Fragmentation of vacuoles happens not only during adaptation to changes in the osmotic environment of the yeast, but also during the cell cycle. The vacuole in the mother cell forms an elongated structure, which extends into the bud and can pinch off tubulovesicular structures (Weisman, 2003). When the bud neck closes, driven by the septins and an actin–myosin ring, these structures are separated from the mother vacuoles, where they fuse again to form the vacuole of the daughter cell (Weisman, 2003). Lack of Fab1p delays this process, whereas cells lacking Vps1p or a functional V-ATPase appear not to be deficient for vacuole inheritance (unpublished observation). The independence of vacuole inheritance from two factors implicated in salt-induced fragmentation suggests that the rather slow fragmentation during cell division may not require all of the factors necessary for the fast adaptation to hyperosmotic shock. Inversely, there are factors necessary for vacuole inheritance that do not influence osmotically induced vacuole fragmentation. In vacuole inheritance, a major force-providing factor for the formation of the thin segregation structures growing out of the vacuole and their migration toward the bud is the myosin-driven transport of vacuoles along actin cables (Hill *et al.*, 1996; Catlett and Weisman, 1998). This factor most likely does not play an active role during osmolarity-induced fragmentation, since we observed that this process is insensitive to the actin depolymerizing drug latrunculin B, as well as to various mutations interfering with actin function (unpublished data).

Careful examination of the morphological changes of the vacuole during salt-induced fragmentation allowed us to dissect the process into two distinct phases with nonoverlapping requirements for the known fragmentation factors. This dissection and the fact that vesiculation happens in an asymmetrical manner at sites that are identifiable in the light microscope provides an important tool for future identification of additional proteins involved in vacuole fragmentation and for studying how they shape the membrane.

MATERIALS AND METHODS

Strains and culture conditions

Culture media were either normal yeast extract/peptone/dextrose (YPD; 2% glucose) or YPD buffered to pH 5.5 (for Δvma strains). Cultures were shaken at 30°C and 150 rpm. Strains carrying expression plasmids were grown on the corresponding Hartwell's Complete dropout medium. Strains used in this study are listed in Table 1. Deletion mutants were generated by replacing the gene with either a loxP-kanMX-loxP cassette from plasmid pUG6 (Guldener *et al.*, 1996) or a nourseothricin (clonNat) cassette from plasmid pFA6a-natNT2 (Janke *et al.*, 2004). Primers used for amplification of those cassettes are as follows: Δfab1, 5′-tcg aat agc aag gta gct tcc ATC CTG TAC ATG CAA GAC CCG TAC GCT GCA GGT CGA C-3′ and 5′-ACC ACG GAT CAG GAA CCA TCA AAA TAT ACC TCT CCA TTG CAT CGA TGA ATT CGA GCT CG-3′ ; Δvac7, 5′-GTA GTA GCA CCT AAT CCT TCT ATT CCC TCT GCC TCC ACA TCC GTA CGC TGC AGG TCG AC-3′ and 5′-CTG GAA TAA ACT CAT CGT GAA GGT TAG TGT GTT GCG GTC GAT CGA TGA ATT CGA GCT CG-3′; Δvac14, 5′-GGT CAA ACA ATG CGT TCT AGA AGG GGA CTA TGA TCG TAT TGC GTA CGC TGC AGG TCG AC-3′ and 5′-CTT TGG CTA ACG GCA CTT TGC GAG ATA TCA GAA TTG GAA TCA TCG ATG AAT TCG AGC TCG-3′; and Δatg18, 5′-ATA GTG TTC CAG TTA ACT CTG TAT CCT TTT CTC TTC GGC CTG ACA CAG CTG AAG CTT CGT ACG C-3′ and 5′-TGC GTT GTG ACG TAC GGA AGG CAG CGC GAG ACA CTT CCG TGA TCA GCA TAG GCC ACT AGT GGA TCT G-3′.

Plasmid construction

The pGEX vector for expression of the glutathione *S*-transferase–tagged double-FYVE finger from mammalian Hrs (Gillooly *et al.*, 2000) was cut with *Eco*RI and *Sal*I and the excised $FYVE_2$-sequence ligated in a pUG36:eGFP vector under the control of a MET25 promoter, resulting in expression of eGFP-$FYVE_2$. The VPH1-GFP plasmid expressing VPH1 under its own promoter has been described previously (Dawaliby and Mayer, 2010), as has the GFP-PHO8 plasmid expressing PHO8 under its endogenous promoter (Baars *et al.*, 2007).

FM4-64 staining

Cells were inoculated from a preculture in stationary phase and grown overnight to logarithmic phase (OD_{600} between 0.2 and 0.8). After dilution to OD_{600} of 0.2 in 2-ml culture, FM4-64 (10 mM in dimethyl sulfoxide [DMSO]) was added to a final concentration of 25 μM. Cells were stained for 1 h, followed by three washing steps (2 min, 3000 × *g*) and a subsequent chase of 1–2 h, depending on the endocytotic efficacy of the strain.

Cell immobilization and fragmentation reaction

Concanavalin A from an aqueous 10 mg/ml stock solution was diluted 10-fold with water. A 35-μl portion was spotted onto LabTek eight-well chambered cover slides and air dried. After the chase period, yeast cells were centrifuged at 2000 × *g* for 3 min and resuspended in 50 μl of fresh medium. A 25-μl portion of the cell suspension were spotted on the previously coated slides and incubated for 5 min. After two washing steps with 400 μl of fresh medium, the cells were kept in 200 μl of medium for imaging. Microscopy was performed at room temperature (22°C). An equal volume of medium containing 1 M NaCl was added during visualization to induce the salt shock. Pictures were taken with an UltraView Vox confocal spinning disk unit (PerkinElmer-Cetus, Waltham, MA) connected to an inverted Zeiss microscope (Carl Zeiss, Jena, Germany) with a 100× oil immersion objective with a numerical aperture of 1.41 and a Hamamatsu C9100-50 camera (Hamamatsu, Hamamatsu, Japan). For colocalization with FM4-64, GFP was excited at 488 nm and imaged using a 527/55-nm bandpass filter. FM4-64 was excited at 488 or at 561 nm for colocalization, respectively. For FRAP analysis, we used the Photokinesis unit of the UltraView Vox system and applied one cycle of 200 ms with full laser intensity at 488 nm to bleach GFP in the target section. Pictures were contrast enhanced with ImageJ (National Institutes of Health, Bethesda, MD) and Photoshop (Adobe, San, Jose, CA). In general, image stacks were recorded at *z*-distances

Strain	Genotype	Source
BJ3505	*MATa pep4::HIS3 prb1-Δ1.6R lys2-208 trp1-Δ*101 ura3-52 gal2 can	Jones *et al*. (1982)
BJ3505 *vps1Δ*	BJ3505; *vps1::kanMX*	Peters *et al*. (2004)
BJ3505 Vph1-GFP	BJ3505; pRS416 VPH1-GFP	This study
BJ3505 *vps1Δ* Vph1-GFP	BJ3505; *vps1::kanMX;* pRS416 VPH1-GFP	This study
BJ3505 GFP-Pho8	BJ3505; pRS316 GFP-PHO8	This study
BJ3505 *vps1Δ* GFP-Pho8	BJ3505; *vps1::kanMX* pRS316 GFP-PHO8	This study
BJ3505 *atg18Δ*	BJ3505; *atg18::natNT2*	This study
CRY1	*MATa ade2-1oc can1-100 his3-11,15 leu2-3112 trp1-1 ura3-1*	Stevens and Davis (1998)
CRY1 soluble GFP	CRY1; pUG36 GFP	This study
DKY6281	*MATα leu2-3 leu2-112 ura3-52 his3-Δ200 trp1-Δ901 lys2-801 suc2-Δ9 pho8::TRP1*	Haas *et al*. (1994)
DKY6281 *vma1Δ*	DKY 6281; *vma1::kanMX*	Bayer *et al*. (2003)
DKY6281 *fab1Δ*	DKY 6281; *fab1::natNT2*	This study
DKY6281 *vac7Δ*	DKY 6281; *vac7::natNT2*	This study
DKY6281 *vac14Δ*	DKY 6281; *vac14::natNT2*	This study
BY4741	MATa his3Δ1 leu2Δ0 met15Δ0 ura3Δ0	EUROSCARF[a]
BY4741 *fab1Δ* FYVE-GFP	BY4741; *fab1::kanMX* (EUROSCARF); pUG36 $FYVE_2$-eGFP	This study
BY4741 *fab1Δ* soluble GFP	BY4741; *fab1::kanMX* (EUROSCARF); pUG36 GFP	This study
AKY106	YPH499; *pep4::URA3*	Kihara *et al*. (2001)
AKY110	AKY106; *vps34::TRP1*	Kihara *et al*. (2001)
AKY112	AKY106; *atg14::LEU2*	Kihara *et al*. (2001)
AKY113	AKY106; *vps38::ADE2*	Kihara *et al*. (2001)
AKY116	AKY106; *vps15::HIS3*	Kihara *et al*. (2001)
BY4733 ADHpr-GFP-Fab1	MATalpha his3Δ200 leu2Δ0 met15Δ0 trp1Δ63 ura3Δ0 FAB1::NatNT2-ADHpr-GFP	C. Ungermann and M. Cabrera (University of Osnabrueck, Osnabrueck Germany)
BY4733 ADHpr-GFP-Fab1 Δatg18	MATalpha his3Δ200 leu2Δ0 met15Δ0 trp1Δ63 ura3Δ0 FAB1::NatNT2-ADHpr-GFP atg18::kanMX	This study

[a]EUROSCARF, European *Saccharomyces cerevisiae* Archive for Functional Analysis, Institute for Molecular Biosciences, Johann Wolfgang Goethe-University Frankfurt, Frankfurt, Germany.

TABLE 1: Yeast strains used in this study.

of 200–500 nm in order to cover the entire depth of the cells. Maximum-intensity projections of the stacks were produced with the ImageJ software and used to evaluate the fragmentation process. The scale bar on all fluorescence pictures corresponds to 5 m.

For quantification of the percentage of cells belonging to three different fragmentation stages, full chips from three independently recorded image series were counted (30–60 cells per picture), resulting in a total of 100–200 cells per strain. The percentage of every class was calculated for every image series, and the mean values and standard deviations were determined from those values. For calculating the surface-to-volume ratio, a total of 15 vacuoles from thee different series were analyzed. Vacuoles were assumed to be spheres. Their diameters in the *xy* plane were measured at least in three different orientations, averaged, and used for calculation.

Concanamycin A treatment

Cells were stained with FM4-64 as described. Concanamycin A was added to the cells at the beginning of the chase period and maintained in all washing steps and on the chambered cover slide. The final concentration of concanamycin A was 2 μM, added from a 200 μM stock in DMSO.

Electron microscopy

Cells were grown in YPD to logarithmic phase. In the morning, they were diluted to $OD_{600\,nm}$ of 0.2 in fresh YPD supplemented with 1% gelatin to improve embedding. Hyperosmotic stress was induced at room temperature by mixing 0.5 ml of cell culture with 0.5 ml of YPD supplemented with 1% gelatin and 1 M NaCl. At different time points after hyperosmotic stress, samples were concentrated by centrifugation (10 s, 2000 × *g*, room temperature), and the pellets were immediately transferred to planchettes of 200-μm depth, cryo-immobilized with HPM 010 high-pressure freezer (Bal-Tec; Leica Microsystems, Buffalo Grove, IL), and stored in liquid nitrogen. Freeze substitution of the samples was carried out in an automated freeze substitution device (Leica Microsystems) in methanol containing 1% OsO_4 (Merck, Darmstadt, Germany) for 24 h at −90°C. Then samples were warmed (5°C/h) to −30°C (3 h) and finally warmed up to 0°C before removal of the substitution medium and embedding

in Epon. Contrasted ultrathin sections (70 nm) were observed in a Tecnai 12 electron microscope (FEI, Eindhoven, Netherlands) operated at 120 keV. Images were taken on an Eagle 4k × 4k camera (FEI) with TIA acquisition software.

ACKNOWLEDGMENTS

We thank Yoshinori Ohsumi, Christian Ungermann, and Margarita Cabrera for strains. We are grateful to Véronique Comte, Monique Reinhardt, and Andrea Schmidt for providing valuable technical assistance and to the Electron Microscopy facility of the University of Lausanne for help in electron microscopy. This work was supported by grants from the SNF (Schweizerischer Nationalfonds) and the ERC (European Research Council) to A.M.

REFERENCES

Acharya U, Mallabiabarrena A, Acharya JK, Malhotra V (1998). Signaling via mitogen-activated protein kinase kinase (MEK1) is required for Golgi fragmentation during mitosis. Cell 92, 183–192.

Baars TL, Petri S, Peters C, Mayer A (2007). Role of the V-ATPase in regulation of the vacuolar fission-fusion equilibrium. Mol Biol Cell 18, 3873–3882.

Bayer MJ, Reese C, Buhler S, Peters C, Mayer A (2003). Vacuole membrane fusion: V0 functions after trans-SNARE pairing and is coupled to the Ca2+-releasing channel. J Cell Biol 162, 211–222.

Bleazard W, McCaffery JM, King EJ, Bale S, Mozdy A, Tieu Q, Nunnari J, Shaw JM (1999). The dynamin-related GTPase Dnm1 regulates mitochondrial fission in yeast. Nat Cell Biol 1, 298–304.

Bonangelino CJ, Nau JJ, Duex JE, Brinkman M, Wurmser AE, Gary JD, Emr SD, Weisman LS (2002). Osmotic stress-induced increase of phosphatidylinositol 3,5-bisphosphate requires Vac14p, an activator of the lipid kinase Fab1p. J Cell Biol 156, 1015–1028.

Botelho RJ, Efe JA, Teis D, Emr SD (2008). Assembly of a Fab1 phosphoinositide kinase signaling complex requires the Fig4 phosphoinositide phosphatase. Mol Biol Cell 19, 4273–4286.

Brett CL, Merz AJ (2008). Osmotic regulation of Rab-mediated organelle docking. Curr Biol 18, 1072–1077.

Burda P, Padilla SM, Sarkar S, Emr SD (2002). Retromer function in endosome-to-Golgi retrograde transport is regulated by the yeast Vps34 PtdIns 3-kinase. J Cell Sci 115, 3889–3900.

Cabrera M, Ostrowicz CW, Mari M, LaGrassa TJ, Reggiori F, Ungermann C (2009). Vps41 phosphorylation and the Rab Ypt7 control the targeting of the HOPS complex to endosome-vacuole fusion sites. Mol Biol Cell 20, 1937–1948.

Catlett NL, Weisman LS (1998). The terminal tail region of a yeast myosin-V mediates its attachment to vacuole membranes and sites of polarized growth. Proc Natl Acad Sci USA 95, 14799–14804.

Chang Y, Schlenstedt G, Flockerzi V, Beck A (2010). Properties of the intracellular transient receptor potential (TRP) channel in yeast, Yvc1. FEBS Lett 584, 2028–2032.

Cooke FT, Dove SK, McEwen RK, Painter G, Holmes AB, Hall MN, Michell RH, Parker PJ (1998). The stress-activated phosphatidylinositol 3-phosphate 5-kinase Fab1p is essential for vacuole function in *S. cerevisiae*. Curr Biol 8, 1219–1222.

Dawaliby R, Mayer A (2010). Microautophagy of the nucleus coincides with a vacuolar diffusion barrier at nuclear-vacuolar junctions. Mol Biol Cell 21, 4173–4183.

Dove SK, Cooke FT, Douglas MR, Sayers LG, Parker PJ, Michell RH (1997). Osmotic stress activates phosphatidylinositol-3,5-bisphosphate synthesis. Nature 390, 187–192.

Dove SK, Dong K, Kobayashi T, Williams FK, Michell RH (2009). Phosphatidylinositol 3,5-bisphosphate and Fab1p/PIKfyve underPPIn endo-lysosome function. Biochem J 419, 1–13.

Dove SK, McEwen RK, Mayes A, Hughes DC, Beggs JD, Michell RH (2002). Vac14 controls PtdIns(3,5)P(2) synthesis and Fab1-dependent protein trafficking to the multivesicular body. Curr Biol 12, 885–893.

Dove SK *et al.* (2004). Svp1p defines a family of phosphatidylinositol 3,5-bisphosphate effectors. EMBO J 23, 1922–1933.

Drose S, Altendorf K (1997). Bafilomycins and concanamycins as inhibitors of V-ATPases and P-ATPases. J Exp Biol 200, 1–8.

Efe JA, Botelho RJ, Emr SD (2007). Atg18 regulates organelle morphology and Fab1 kinase activity independent of its membrane recruitment by phosphatidylinositol 3,5-bisphosphate. Mol Biol Cell 18, 4232–4244.

Farge E, Devaux PF (1992). Shape changes of giant liposomes induced by an asymmetric transmembrane distribution of phospholipids. Biophys J 61, 347–357.

Gary JD, Sato TK, Stefan CJ, Bonangelino CJ, Weisman LS, Emr SD (2002). Regulation of Fab1 phosphatidylinositol 3-phosphate 5-kinase pathway by Vac7 protein and Fig4, a polyphosphoinositide phosphatase family member. Mol Biol Cell 13, 1238–1251.

Gary JD, Wurmser AE, Bonangelino CJ, Weisman LS, Emr SD (1998). Fab1p is essential for PtdIns(3)P 5-kinase activity and the maintenance of vacuolar size and membrane homeostasis. J Cell Biol 143, 65–79.

Gillooly DJ, Morrow IC, Lindsay M, Gould R, Bryant NJ, Gaullier JM, Parton RG, Stenmark H (2000). Localization of phosphatidylinositol 3-phosphate in yeast and mammalian cells. EMBO J 19, 4577–4588.

Gomes de Mesquita DS, van den Hazel HB, Bouwman J, Woldringh CL (1996). Characterization of new vacuolar segregation mutants, isolated by screening for loss of proteinase B self-activation. Eur J Cell Biol 71, 237–247.

Guldener U, Heck S, Fielder T, Beinhauer J, Hegemann JH (1996). A new efficient gene disruption cassette for repeated use in budding yeast. Nucleic Acids Res 24, 2519–2524.

Haas A, Conradt B, Wickner W (1994). G-protein ligands inhibit in vitro reactions of vacuole inheritance. J Cell Biol 126, 87–97.

Haas A, Scheglmann D, Lazar T, Gallwitz D, Wickner W (1995). The GTPase Ypt7p of Saccharomyces cerevisiae is required on both partner vacuoles for the homotypic fusion step of vacuole inheritance. EMBO J 14, 5258–5270.

Hamill OP, Martinac B (2001). Molecular basis of mechanotransduction in living cells. Physiol Rev 81, 685–740.

Henriquez R, Blobel G, Aris JP (1990). Isolation and sequencing of NOP1. A yeast gene encoding a nucleolar protein homologous to a human autoimmune antigen. J Biol Chem 265, 2209–2215.

Hill KL, Catlett NL, Weisman LS (1996). Actin and myosin function in directed vacuole movement during cell division in Saccharomyces cerevisiae. J Cell Biol 135, 1535–1549.

Hinshaw JE (2000). Dynamin and its role in membrane fission. Annu Rev Cell Dev Biol 16, 483–519.

Hothorn M *et al.* (2009). Catalytic core of a membrane-associated eukaryotic polyphosphate polymerase. Science 324, 513–516.

Janke C *et al.* (2004). A versatile toolbox for PCR-based tagging of yeast genes, new fluorescent proteins, more markers and promoter substitution cassettes. Yeast 21, 947–962.

Jin N *et al.* (2008). VAC14 nucleates a protein complex essential for the acute interconversion of PI3P and PI(3,5)P(2) in yeast and mouse. EMBO J 27, 3221–3234.

Jones EW, Zubenko GS, Parker RR (1982). PEP4 gene function is required for expression of several vacuolar hydrolases in *Saccharomyces cerevisiae*. Genetics 102, 665–677.

Julicher F, Lipowsky R (1993). Domain-induced budding of vesicles. Phys Rev Lett 70, 2964–2967.

Kametaka S, Okano T, Ohsumi M, Ohsumi Y (1998). Apg14p and Apg6/Vps30p form a protein complex essential for autophagy in the yeast, *Saccharomyces cerevisiae*. J Biol Chem 273, 22284–22291.

Kane PM (2007). The long physiological reach of the yeast vacuolar H+-ATPase. J Bioenerg Biomembr 39, 415–421.

Kihara A, Noda T, Ishihara N, Ohsumi Y (2001). Two distinct Vps34 phosphatidylinositol 3-kinase complexes function in autophagy and carboxypeptidase Y sorting in *Saccharomyces cerevisiae*. J Cell Biol 152, 519–530.

Kuravi K, Nagotu S, Krikken AM, Sjollema K, Deckers M, Erdmann R, Veenhuis M, van der Klei IJ (2006). Dynamin-related proteins Vps1p and Dnm1p control peroxisome abundance in *Saccharomyces cerevisiae*. J Cell Sci 119, 3994–4001.

LaGrassa TJ, Ungermann C (2005). The vacuolar kinase Yck3 maintains organelle fragmentation by regulating the HOPS tethering complex. J Cell Biol 168, 401–414.

Li SC, Diakov TT, Rizzo JM, Kane PM (2012). The V-ATPase works in parallel with the HOG pathway to adapt *Saccharomyces cerevisiae* cells to osmotic stress. Eukaryot Cell 11, 282–291.

Lipowsky R (1995). The morphology of lipid membranes. Curr Opin Struct Biol 5, 531–540.

Liss E, Langen P (1962). Experiments on polyphosphate overcompensation in yeast cells after phosphate deficiency [in German]. Arch Mikrobiol 41, 383–392.

Mayer A, Wickner W (1997). Docking of yeast vacuoles is catalyzed by the Ras-like GTPase Ypt7p after symmetric priming by Sec18p (NSF). J Cell Biol 136, 307–317.

Michaillat L, Baars TL, Mayer A (2012). Cell-free reconstitution of vacuole membrane fragmentation reveals regulation of vacuole size and number by TORC1. Mol Biol Cell 23, 881–895.
Mui BL, Dobereiner HG, Madden TD, Cullis PR (1995). Influence of transbilayer area asymmetry on the morphology of large unilamellar vesicles. Biophys J 69, 930–941.
Muller O, Bayer MJ, Peters C, Andersen JS, Mann M, Mayer A (2002). The Vtc proteins in vacuole fusion: coupling NSF activity to V(0) trans-complex formation. EMBO J 21, 259–269.
Muller O, Neumann H, Bayer MJ, Mayer A (2003). Role of the Vtc proteins in V-ATPase stability and membrane trafficking. J Cell Sci 116, 1107–1115.
Muller O, Sattler T, Flotenmeyer M, Schwarz H, Plattner H, Mayer A (2000). Autophagic tubes: vacuolar invaginations involved in lateral membrane sorting and inverse vesicle budding. J Cell Biol 151, 519–528.
Pan X, Roberts P, Chen Y, Kvam E, Shulga N, Huang K, Lemmon S, Goldfarb DS (2000). Nucleus-vacuole junctions in *Saccharomyces cerevisiae* are formed through the direct interaction of Vac8p with Nvj1p. Mol Biol Cell 11, 2445–2457.
Peplowska K, Markgraf DF, Ostrowicz CW, Bange G, Ungermann C (2007). The CORVET tethering complex interacts with the yeast Rab5 homolog Vps21 and is involved in endo-lysosomal biogenesis. Dev Cell 12, 739–750.
Peters C, Baars TL, Buhler S, Mayer A (2004). Mutual control of membrane fission and fusion proteins. Cell 119, 667–678.
Peters C, Bayer MJ, Buhler S, Andersen JS, Mann M, Mayer A (2001). Trans-complex formation by proteolipid channels in the terminal phase of membrane fusion. Nature 409, 581–588.
Praefcke GJ, McMahon HT (2004). The dynamin superfamily: universal membrane tubulation and fission molecules?. Nat Rev Mol Cell Biol 5, 133–147.
Rao NN, Gomez-Garcia MR, Kornberg A (2009). Inorganic polyphosphate: essential for growth and survival. Annu Rev Biochem 78, 605–647.
Rothlisberger S, Jourdain I, Johnson C, Takegawa K, Hyams JS (2009). The dynamin-related protein Vps1 regulates vacuole fission, fusion and tubulation in the fission yeast, *Schizosaccharomyces pombe*. Fungal Genet Biol 46, 927–935.
Rothman JH, Raymond CK, Gilbert T, O'Hara PJ, Stevens TH (1990). A putative GTP binding protein homologous to interferon-inducible Mx proteins performs an essential function in yeast protein sorting. Cell 61, 1063–1074.
Roux A, Koster G, Lenz M, Sorre B, Manneville JB, Nassoy P, Bassereau P (2010). Membrane curvature controls dynamin polymerization. Proc Natl Acad Sci USA 107, 4141–4146.
Sackmann E, Feder T (1995). Budding, fission and domain formation in mixed lipid vesicles induced by lateral phase separation and macromolecular condensation. Mol Membr Biol 12, 21–28.
Sattler T, Mayer A (2000). Cell-free reconstitution of microautophagic vacuole invagination and vesicle formation. J Cell Biol 151, 529–538.
Schaffer E, Thiele U (2004). Dynamic domain formation in membranes: thickness-modulation-induced phase separation. Eur Phys J E Soft Matter 14, 169–175.
Schmid SL, Frolov VA (2011). Dynamin: functional design of a membrane fission catalyst. Annu Rev Cell Dev Biol 27, 79–105.
Schu PV, Takegawa K, Fry MJ, Stack JH, Waterfield MD, Emr SD (1993). Phosphatidylinositol 3-kinase encoded by yeast VPS34 gene essential for protein sorting. Science 260, 88–91.
Sethuraman A, Rao NN, Kornberg A (2001). The endopolyphosphatase gene: essential in *Saccharomyces cerevisiae*. Proc Natl Acad Sci USA 98, 8542–8547.
Shi X, Kornberg A (2005). Endopolyphosphatase in *Saccharomyces cerevisiae* undergoes post-translational activations to produce short-chain polyphosphates. FEBS Lett 579, 2014–2018.
Smaczynska-de Rooij II, Allwood EG, Aghamohammadzadeh S, Hettema EH, Goldberg MW, Ayscough KR (2010). A role for the dynamin-like protein Vps1 during endocytosis in yeast. J Cell Sci 123, 3496–3506.
Stevens RC, Davis TN (1998). Mlc1p is a light chain for the unconventional myosin Myo2p in *Saccharomyces cerevisiae*. J Cell Biol 142, 711–722.
Stromhaug PE, Reggiori F, Guan J, Wang CW, Klionsky DJ (2004). Atg21 is a phosphoinositide binding protein required for efficient lipidation and localization of Atg8 during uptake of aminopeptidase I by selective autophagy. Mol Biol Cell 15, 3553–3566.
Tang F, Kauffman EJ, Novak JL, Nau JJ, Catlett NL, Weisman LS (2003). Regulated degradation of a class V myosin receptor directs movement of the yeast vacuole. Nature 422, 87–92.
Tsukada M, Ohsumi Y (1993). Isolation and characterization of autophagy-defective mutants of *Saccharomyces cerevisiae*. FEBS Lett 333, 169–174.
Uttenweiler A, Schwarz H, Neumann H, Mayer A (2007). The vacuolar transporter chaperone (VTC) complex is required for microautophagy. Mol Biol Cell 18, 166–175.
Vater CA, Raymond CK, Ekena K, Howald-Stevenson I, Stevens TH (1992). The VPS1 protein, a homolog of dynamin required for vacuolar protein sorting in *Saccharomyces cerevisiae*, is a GTPase with two functionally separable domains. J Cell Biol 119, 773–786.
Vida TA, Emr SD (1995). A new vital stain for visualizing vacuolar membrane dynamics and endocytosis in yeast. J Cell Biol 128, 779–792.
Wada Y, Ohsumi Y, Anraku Y (1992). Genes for directing vacuolar morphogenesis in *Saccharomyces cerevisiae*. I. Isolation and characterization of two classes of vam mutants. J Biol Chem 267, 18665–18670.
Wang YX, Zhao H, Harding TM, Gomes de Mesquita DS, Woldringh CL, Klionsky DJ, Munn AL, Weisman LS (1996). Multiple classes of yeast mutants are defective in vacuole partitioning yet target vacuole proteins correctly. Mol Biol Cell 7, 1375–1389.
Ward DM, Leslie JD, Kaplan J (1997). Homotypic lysosome fusion in macrophages: analysis using an in vitro assay. J Cell Biol 139, 665–673.
Weisman LS (2003). Yeast vacuole inheritance and dynamics. Annu Rev Genet 37, 435–460.
Wichmann H, Hengst L, Gallwitz D (1992). Endocytosis in yeast: evidence for the involvement of a small GTP-binding protein (Ypt7p). Cell 71, 1131–1142.
Wurmser AE, Emr SD (1998). Phosphoinositide signaling and turnover: PtdIns(3)P, a regulator of membrane traffic, is transported to the vacuole and degraded by a process that requires lumenal vacuolar hydrolase activities. EMBO J 17, 4930–4942.
Yamamoto A, DeWald DB, Boronenkov IV, Anderson RA, Emr SD, Koshland D (1995). Novel PI(4)P 5-kinase homologue, Fab1p, essential for normal vacuole function and morphology in yeast. Mol Biol Cell 6, 525–539.
Yu X, Cai M (2004). The yeast dynamin-related GTPase Vps1p functions in the organization of the actin cytoskeleton via interaction with Sla1p. J Cell Sci 117, 3839–3853.